

Article

# Effects of Terrain Parameters and Spatial Resolution of a Digital Elevation Model on the Calculation of Potential Solar Radiation in the Mountain Environment: A Case Study of the Tatra Mountains

Renata Ďuračiová \*  and Filip Pružinec

Department of Theoretical Geodesy and Geoinformatics, Faculty of Civil Engineering,  
Slovak University of Technology in Bratislava, 810 05 Bratislava, Slovakia; filip.pruzinec@stuba.sk

\* Correspondence: renata.duraciova@stuba.sk

**Abstract:** Solar radiation significantly affects many processes on Earth. In situ measurements are demanding and require a dense network of sensors. A suitable alternative solution could be the modelling of potential solar radiation based on a digital elevation model (DEM) in geographic information systems. The key issue of this study is to determine the influence of the terrain parameters and the spatial resolution of a DEM on the calculation of potential solar radiation. The area of study is the Tatra Mountains (the highest mountains of the Carpathians). The DEM determined from light detection and ranging (LiDAR) was used. To determine the influence of the terrain, the following terrain parameters were applied: slope; aspect, represented by northness and eastness; elevation; and topographical position index using six different circular neighbourhoods (10 m, 30 m, 50 m, 100 m, 500 m, and 1000 m). The results indicate a moderate correlation (0.32–0.46) between the solar radiation calculation errors and the absolute values of the topographic position indices with small neighbourhoods (10 m–100 m). To show the impact of the spatial resolution, the calculation was performed based on four different DEM resolutions, namely 5 m, 10 m, 30 m, and 90 m. Mutual differences in potential solar radiation were quantified concerning the topographic position index. The result is also a model of potential annual solar radiation in the Tatra Mountains, calculated at a resolution of 5 m or 2 m.

**Keywords:** potential solar radiation; LiDAR; digital elevation model resolution; topographical position index; geographical information system; Carpathians; Slovakia



**Citation:** Ďuračiová, R.; Pružinec, F. Effects of Terrain Parameters and Spatial Resolution of a Digital Elevation Model on the Calculation of Potential Solar Radiation in the Mountain Environment: A Case Study of the Tatra Mountains. *ISPRS Int. J. Geo-Inf.* **2022**, *11*, 389. <https://doi.org/10.3390/ijgi11070389>

Academic Editors: Sisi Zlatanova and Wolfgang Kainz

Received: 11 March 2022

Accepted: 8 July 2022

Published: 11 July 2022

**Publisher's Note:** MDPI stays neutral with regard to jurisdictional claims in published maps and institutional affiliations.



**Copyright:** © 2022 by the authors. Licensee MDPI, Basel, Switzerland. This article is an open access article distributed under the terms and conditions of the Creative Commons Attribution (CC BY) license (<https://creativecommons.org/licenses/by/4.0/>).

## 1. Introduction

Solar radiation is a general term for the electromagnetic radiation emitted by the Sun [1]. It is a source of energy and significantly affects the environment, as well as geological and natural processes and the health and vitality of humans, animals, and plants [2–5]. It is also an important renewable energy source that helps sustain life on Earth. Solar energy can be actively used to generate electricity in power plants but also passively to generate electricity using photovoltaic systems on the roofs and facades of buildings. To optimize the distribution of these devices, it is necessary to know the distribution of solar radiation in the country. Because solar radiation is essential for plant growth, knowledge of its distribution also helps, for example, in planning the cultivation or protection of sun-demanding plants. In the mountain environment, it is specifically a matter of forest protection. Another application in the mountain environment, where it is necessary to know the distribution of solar radiation, is the prediction of avalanche hazards.

Solar radiation that hits the georelief is the result of a complex interaction between the atmosphere and the Earth's surface. Its amount depends on many factors, for example, geographic location, season, time of day, local landscape, cloud cover, and other optical

properties of the atmosphere [6]. In the case of considerable vertical fragmentation of the area, direct measurements are insufficient to express the spatial and temporal variability of solar radiation incidents on the surface of the georelief [7,8]. Although there are thousands of solar radiation monitoring stations around the world, for most geographic areas, there is no accurate data available on solar radiation [9]. Management of measurements in a mountain environment is even more problematic due to difficult access to rugged terrain. In situ measurements are also demanding and require a dense network of sensors. Therefore, in addition to the available measurements, it is necessary to use existing knowledge and create suitable models of solar radiation. Because modelling the influence of local weather on solar radiation modelling is very demanding and inaccurate, potential solar radiation is often calculated based on digital elevation models (DEMs) [10,11]. This is also due to the fact that many analyses require modelling of potential solar radiation with sufficient positional accuracy, albeit with lower temporal accuracy. In addition, for many spatial analyses, the value of solar radiation at a certain point in relation to its surroundings is often more important than absolutely accurate values in the whole area. A suitable parameter that meets these requirements is potential annual solar radiation calculated at high spatial resolution in geographical information systems (GIS).

The main spatial distribution factor of potential solar radiation is georelief, especially elevation, slope, and aspect. This paper is therefore devoted to determining the effect of the used DEM resolution, as well as the above-mentioned terrain parameters, on the calculation of potential solar radiation in GIS.

Currently, the most used software tools for the calculation of potential solar radiation are the Solar Radiation toolset implemented in ArcGIS [12,13] and r.sun [14], which was designed for the GRASS GIS [15]. Selected studies that describe the implementation of calculation of solar radiation based on 3D data are also presented in [9]. The article [9] states that one of the main models created in a GIS tool is Solar Analyst, developed by Fu and Rich [16–20] based on a theory called SolarFlux. The model was created as a module in ArcView 3.0 software created by ESRI (Environmental Systems Research Institute) and later implemented in the ArcGIS 10 extension known as the Solar Radiation toolset [12,13].

Many articles have been devoted to the calculation of potential solar radiation. Some of them focus on fundamental research of the calculation of potential solar radiation [5,21–24]; others focus on its use in various applications [8,25–33]. For example, [8] is devoted to the calibration and validation of the ArcGIS Solar Radiation tools for photovoltaic potential determination, focusing mainly on the input atmospheric parameters, diffusivity, and transmissivity but also pointing to the importance of spatial resolution in the calculation of potential solar radiation. According to [8], most GIS-based methods for calculating solar radiation are based on some form of geographic data, such as DEMs [10,11,21,22] or light detection and ranging (LiDAR) data [5,24–28]. These methods also use different assumptions and therefore differ in terms of accuracy and performance [8]. For example, refs [5,24,25,28] describe tools for calculating potential solar radiation from 3D LiDAR data.

In the field of applications and uses of calculated potential solar radiation in mountain areas, the effect of solar radiation on forest damage by bark beetle attacks was described in some papers [34–41]. Specifically, in [30,39,40], potential solar radiation was applied as one of the site characteristics in the determination of the probability of bark beetle attack in the Tatra Mountains. In [30], the authors stated that potential solar radiation calculated based on the DEM better identified beetle infestations than commonly used meteorological variables. However, it should be emphasized that DEM at a resolution of 30 m (e.g., based on shuttle radar topography mission (SRTM) [41–43]) was mostly used in those analyses.

Although the influence of the DEM resolution on the calculation of potential solar radiation is known to be significant [8,10,11], it has not yet been quantified how accurate the input DEM should be or which error in the calculation of potential solar radiation would result from using a lower-quality DEM. The authors mostly point to different DEMs, which means that the results also show a difference resulting from another data source. In this study, we used only one data source and aggregated it by the average function to different

resolutions. This leads to a real indication of the influence of the DEM spatial resolution on the calculation of potential solar radiation. We used an available DEM derived from LiDAR data.

Another issue is how terrain fragmentation affects the accuracy of the calculation, although we can assume that differences in potential solar radiation are more significant in mountainous environments. Therefore, the aim is also to determine the influence of terrain parameters on errors in the calculated potential radiation caused by the lower resolution of the input data. Because the values of solar radiation change most in rugged terrain, we focused mainly on the mountain environment, specifically on the Slovak side of the Tatra Mountains (the highest mountains of the Carpathians).

We assume that based on the results, we will be able to better determine in which areas it is important to use a DEM with higher resolution and where a lower resolution is sufficient to model potential solar radiation. In the experiment, we tested DEM resolutions of 5 m, 10 m, 30 m, and 90 m.

This paper is further organized as follows. Section 2 describes the data and methods used, including a description of the study area, available data sources, the design of the experiment, and a description of the software tools used. Section 3 presents the results of quantifying the effects of DEM resolution on the calculation of potential solar radiation, as well as correlations between terrain parameters and errors in the calculation of potential solar radiation caused by lower spatial resolution. Section 4 provides a discussion of the results, and Section 5 concludes the document.

## 2. Materials and Methods

### 2.1. Study Area

The study area is located in the Tatra Mountains (Central Europe), the highest range within the Carpathians, located on the border between Poland and Slovakia (Figure 1). In 1949, the Tatra Mountains were declared the first national park in Slovakia (TANAP), and in 1993, together with the Polish part of the Tatras, they were declared the “Biosphere Reserve of the Tatras” by UNESCO [44]. The High Tatras include as many as 30 peaks more than 2500 m above sea level (a.s.l.), with the elevation reaching 2655 m a.s.l. (Gerlach). The Tatra Mountains are characterized by deep valleys and mountain ridges, so they are very suitable for performing an analysis of the effects of georelief on the calculation of potential solar radiation. The study area has a west–east elongated shape (Figure 1), and its area is 959 km<sup>2</sup>, corresponding to zone 26 from LiDAR data provided by the Geodesy Cartography and Cadastre Authority of the Slovak Republic (GCCA SR; the abbreviation in Slovak used to denote data is ÚGKK SR) [45] (Figure 2).

### 2.2. Data

For the Slovak side of the Tatra Mountains, solar radiation data are partly provided by the Slovak Hydrometeorological Institute [48]. Unfortunately, the network of ground stations is not dense enough for precise spatial analysis, and measurements are relatively expensive. The data on solar radiation is also provided, for example, by Global Solar Atlas [49]. These data are very good in terms of temporal accuracy and also consider meteorological conditions. However, their spatial resolution (pixel size: 250 m) is not sufficient for detailed spatial analysis. Therefore, it is more appropriate to use calculated potential solar radiation for many spatial analyses with higher spatial resolution. The calculation of potential solar radiation is based on DEM. In spatial analysis in the Tatra Mountains, SRTM [43] with a resolution of 10 m or more has been an available and often used DEM. However, since 2017, the GCCA SR has been continuously creating and providing a digital terrain model, DTM 5.0, and digital surface model, DSM 1.0, of the entire territory of the Slovak Republic [45]. The DTM 5.0 and DSM 1.0 models were created from aerial laser scanning (ALS) data, and the declared density of the data is at least five points per m<sup>2</sup>. Both models are provided in raster format at a spatial resolution of 1 m. The whole territory of the Slovak Republic is divided into 42 localities (Figure 2).

Scanning takes place gradually in individual locations from the west of Slovakia to the east. Available areas for users are highlighted in green in Figure 2. Number 26 indicates the study area. The parameters of ALS data collection from area 26 (Tatras) are presented in Table 1. We assume that these data provide a suitable basis for more accurate modelling of potential solar radiation.

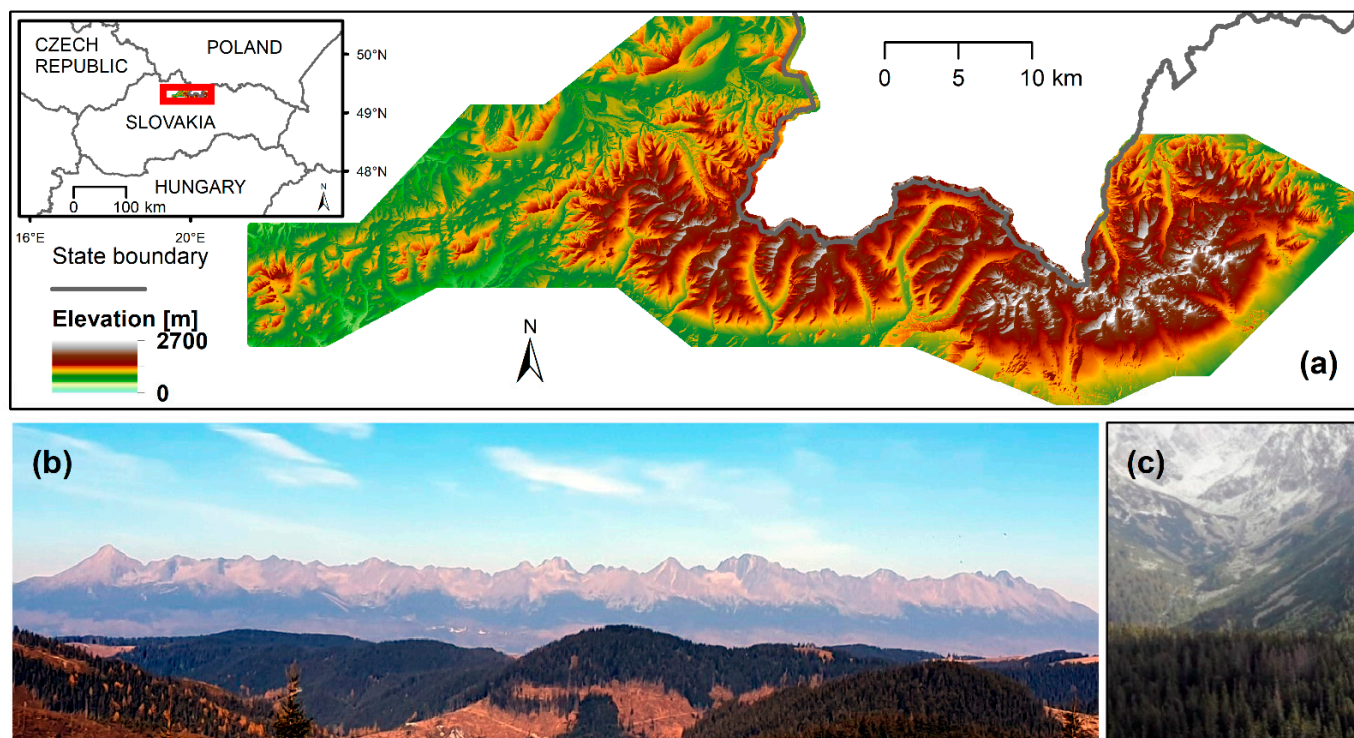


**Figure 1.** (a) Study area: Slovak part of the Tatra Mountains in the range of zone 26 of LiDAR data provided by [45]. Data sources: ÚGKK SR [45], © OpenStreetMap contributors [46,47]. (b) View of the study area (photographed from the Low Tatras). (c) Local view. Photo: R. Ď.

**Table 1.** The parameters of ALS data collection from the study area (number 26: Tatras). Data source: [51].

Parameter	Value
Number	26
Name	Tatras
Area [km <sup>2</sup> ]	959
Scanning period	7 June 2018–12 September 2018
Altitude accuracy of the point cloud in ETRS89-h (m)	0.04
Position accuracy of the point cloud in ETRS89-TM-34 (m)	0.17
Average density of points of the last reflection (points/m <sup>2</sup> )	30
Altitude accuracy of DTM 5.0 in Bpv <sup>1</sup> (m)	0.04

<sup>1</sup> Altitude reference system used in Slovakia.

The data are freely available, but the user is obliged to state the source of ALS products when creating his own work and publishing it as follows: “ÚGKK SR”. Data from smaller areas (up to 400 km<sup>2</sup>) can also be downloaded via the ZBGIS Map Client application [50] (Figure 2). In this case study, we used DTM 5.0 aggregated to a resolution of 5 m. Because DTM 5.0 is the name of a specific model that could be replaced by another DEM in our study, we prefer to use the general abbreviation DEM hereafter. We use the abbreviation DTM 5.0 only if we want to emphasize this model specifically.

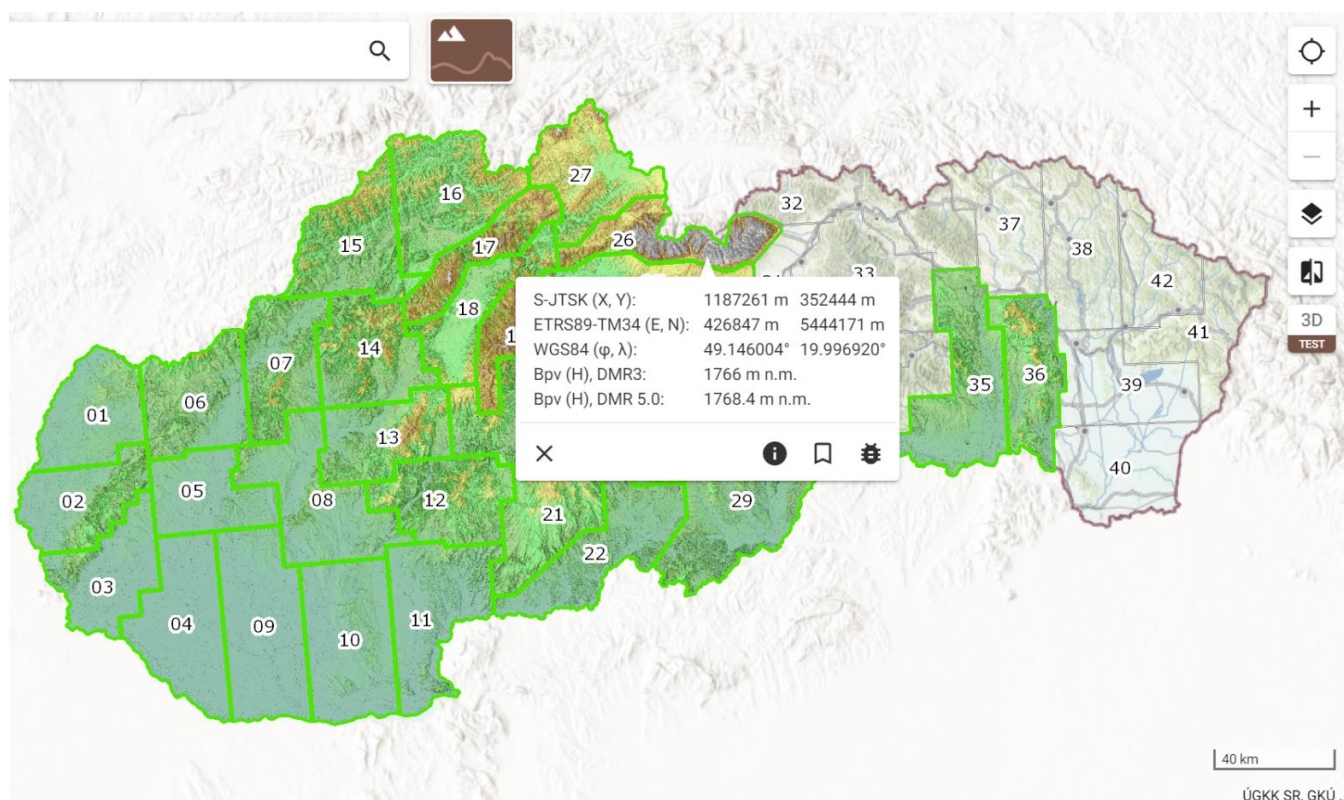


**Figure 2.** The ZBGIS Map Client application provided by the GCCA SR (ÚGKK SR). Areas from which DTM 5.0 data are available are highlighted in green. Source: [50].

### 2.3. Experimental Design

In an experiment, we compared potential solar radiation calculated at the resolution corresponding to SRTM (10 m or 30 m) or lower (90 m) with values calculated at a finer resolution (5 m). We chose resolutions 3 times higher and 3 lower than the resolution of the commonly used SRTM model in the study area. The highest resolution used (5 m) was one with which it was possible to perform each of the designed and implemented calculations in the ArcGIS environment in a relatively short time (in this case, within two days). We used DTM 5.0 data aggregated from the original resolution of 1 m to a resolution of 5 m, 10 m, 30 m, and 90 m because we wanted to emphasize the effect of the input resolution used, not the DEM differences. Raster aggregation generates a reduced-resolution version of a raster. In this case, we used the aggregation function Mean. Therefore, each output cell contains the mean of the input cells that are encompassed by the extent of that cell. Therefore, we included all values from the original raster in the calculation, which is an advantage compared to using one of a resampling method, such as Nearest, Majority, Bilinear, or Cubic [52]. Using aggregation, we later also created models of potential solar radiation with resolutions of 10 m, 30 m, and 90 m. We aggregated them from a model calculated with a resolution of 5 m. For the above reason, we assume that it is more appropriate than calculating them directly at a lower resolution. We emphasize that our aim is to point out the effect of terrain parameters and spatial resolution of DEM on the calculation of potential solar radiation, not to calculate potential solar radiation as accurately as possible. Four different resolutions are sufficient for this purpose. We did not use the raster with the original resolution of 1 m due to the computational complexity of determining the potential solar radiation in such a large area. A model with a resolution of 2 m can also be calculated, but the calculation can take more than 10 days.

To assess the impact of terrain, we calculated the terrain parameters (aspect and slope) and the derived terrain parameters, such as northness, eastness [53], and topographic position indices (TPIs) [54,55]. TPIs compares the elevation of each cell in a DEM to the

mean elevation of a specified neighbourhood around that cell [52]. Although aspect is an important terrain parameter, it is difficult to include it directly in the analysis due to its angular scale ( $0^\circ$  to  $360^\circ$ , with values  $0^\circ$  and  $360^\circ$  being close to each other). Therefore, we suggest using the parameters of northness ( $northness = \cos(aspect)$ ) and eastness ( $eastness = \sin(aspect)$ ) [53] instead of aspect. The slope is expressed in degrees but only in the range of  $0^\circ$  to  $90^\circ$ , so we included it in the analysis in this form. To better express terrain edges and extremes, we suggest applying absolute values of TPI (i.e., we do not distinguish whether it is a higher or lower position of points, and only mutual differences are important). All parameters were calculated based on DTM 5.0 [45] at a spatial resolution of 5 m.

We subsequently calculated the correlations of the terrain parameters with the differences in potential solar radiation calculated at various resolutions. To exclude values from marginal areas, which may be inaccurate due to incomplete marginal input data, we excluded from the comparison the zone up to 200 m. Finally, we compared the calculated and aggregated values of potential annual solar radiation at multiple resolutions. The simplified experimental procedure is shown in Figure 3.

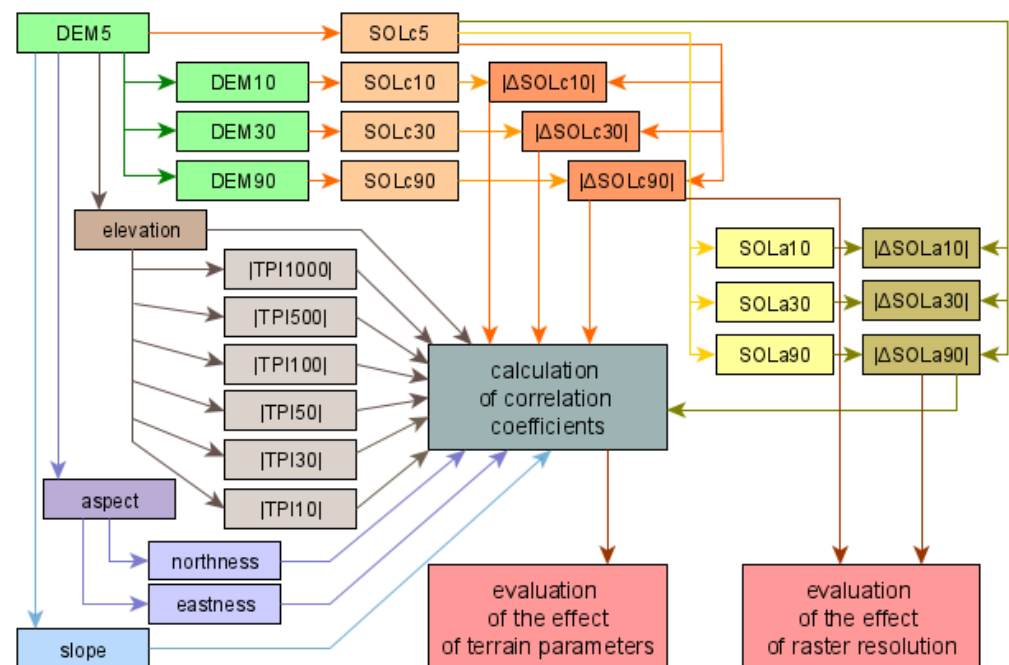


**Figure 3.** The design of an experiment to assess the effects of terrain parameters and spatial resolution of DEM on the calculation of potential solar radiation: DEM $x$ —DEM with a spatial resolution of  $x$  m; SOL $c$  $x$ —potential solar radiation *calculated* from DEM at a resolution of  $x$  m; SOL $a$  $x$ —potential solar radiation *aggregated* at a resolution of  $x$  m;  $|\Delta SOLcx|$  /  $|\Delta SOLax|$ —the absolute value of the difference between the values of SOL $c$ 5 and the values of potential solar radiation *calculated/aggregated* at a resolution of  $x$  m;  $|TPIy|$ —topographic position index calculated with a neighbourhood of  $y$  m.

#### 2.4. Software Tools and Data Processing

We calculated potential annual global solar radiation in the ArcGIS 10.8 software environment using the Area Solar Radiation tool (implemented in the Solar Radiation toolset) [12,13]. This tool calculates potential solar radiation over a geographic area based on the hemispherical viewshed algorithm explained in [18,19]. The total amount of radiation is calculated for a given location in units of  $Wh/m^2$  [12,13]. The Area Solar Radiation tool takes location (latitude–longitude), elevation, slope, aspect, and atmospheric transmission as the most relevant inputs [8,13]. These parameters usually result from the input data. Other input settings are listed in Table 2. We used default values, except for latitude, which was automatically calculated for the site area.

**Table 2.** Input parameters used for calculation of solar radiation using the Area Solar Radiation tool.

Input Parameter	Value
Latitude (°)	49.21231
Sky size/resolution	200
Day interval	14
Hour interval	2
Calculation directions	32
Zenith divisions	8
Diffuse model type	UNIFORM SKY
Diffuse proportion	0.3
Transmissivity	0.5

For calculation of the terrain parameters and parameters derived from them, we used standard tools, such as Aspect, Slope, Focal Statistics, and Raster Calculator (Spatial Analyst) in ArcGIS 10.8 [56]. The input data representing variables were used in raster form at a spatial resolution of 5 m.

### 3. Results

The results of the analysis can be summarized in several points:

- (1) Differences in potential annual solar radiation calculated at resolutions of 10 m, 30 m, and 90 m compared to potential annual solar radiation calculated at a resolution of 5 m, supplemented by their statistical characteristics;
- (2) Correlations between absolute values of potential solar radiation differences and the terrain parameters to assess the influence of terrain fragmentation on the accuracy of the calculation of potential solar radiation;
- (3) Comparison of calculated and aggregated models of potential annual solar radiation;
- (4) The model of annual potential solar radiation in the Tatra Mountains with a cell size of 5 m (or 2 m), which is applicable in various spatial analyses.

#### 3.1. Differences in Potential Annual Solar Radiation Calculated at Different Resolutions

Table 3 contains the statistical characteristics (minimum, maximum, mean, and root mean square error (RMSE)) of the calculated differences in solar radiation at a resolution of 5 m compared to the potential solar radiation calculated at a resolution of 10 m, 30 m, and 90 m. The differences in potential annual solar radiation calculated at a resolution of 30 m compared to potential annual solar radiation calculated at a resolution of 5 m are shown in Figure 4a,b. Figure 4c shows TPI calculated with a circular neighbourhood of 100 m (TPI100) and illustrates, in detail, the relationship between the calculated differences shown in Figure 4a,b and TPI100.

**Table 3.** Statistical characteristics (minimum, maximum, mean, and RMSE) of the differences in potential solar radiation calculated at different resolutions.

Difference [Wh/m <sup>2</sup> ]	Min [Wh/m <sup>2</sup> ]	Max [Wh/m <sup>2</sup> ]	Mean [Wh/m <sup>2</sup> ]	RMSE [Wh/m <sup>2</sup> ]
$\Delta_{5-10}$ <sup>1</sup>	−1,084,673.1	969,098.8	−5608.4	43,064.0
$\Delta_{5-30}$ <sup>1</sup>	−1,316,829.5	1,083,598.8	−18,166.1	75,813.2
$\Delta_{5-90}$ <sup>1</sup>	−1,364,494.3	1,047,376.5	−40,078.0	117,945.2

<sup>1</sup>  $\Delta_{5-10}$ ,  $\Delta_{5-30}$ , and  $\Delta_{5-90}$  indicate the difference in potential solar radiation calculated at a resolution of 5 m compared to potential solar radiation calculated at a resolution of 10 m, 30 m, and 90 m, respectively.

It is also important to note that the processing time increases significantly with increasing raster resolution. In our study, the processing times were 0 m: 21 s; 3 m: 29 s; 48 m: 42 s; 24 h: 14 m: 08 s; and 11 d: 14 h: 04 m at a resolution of 90 m, 30 m, 10 m, 5 m, and 2 m, respectively. The study area is 959 m<sup>2</sup>, and processing was performed on a Windows 10 computer with an Intel 11th Generation Core i9 processor with 16 cores and 32 GB of RAM.

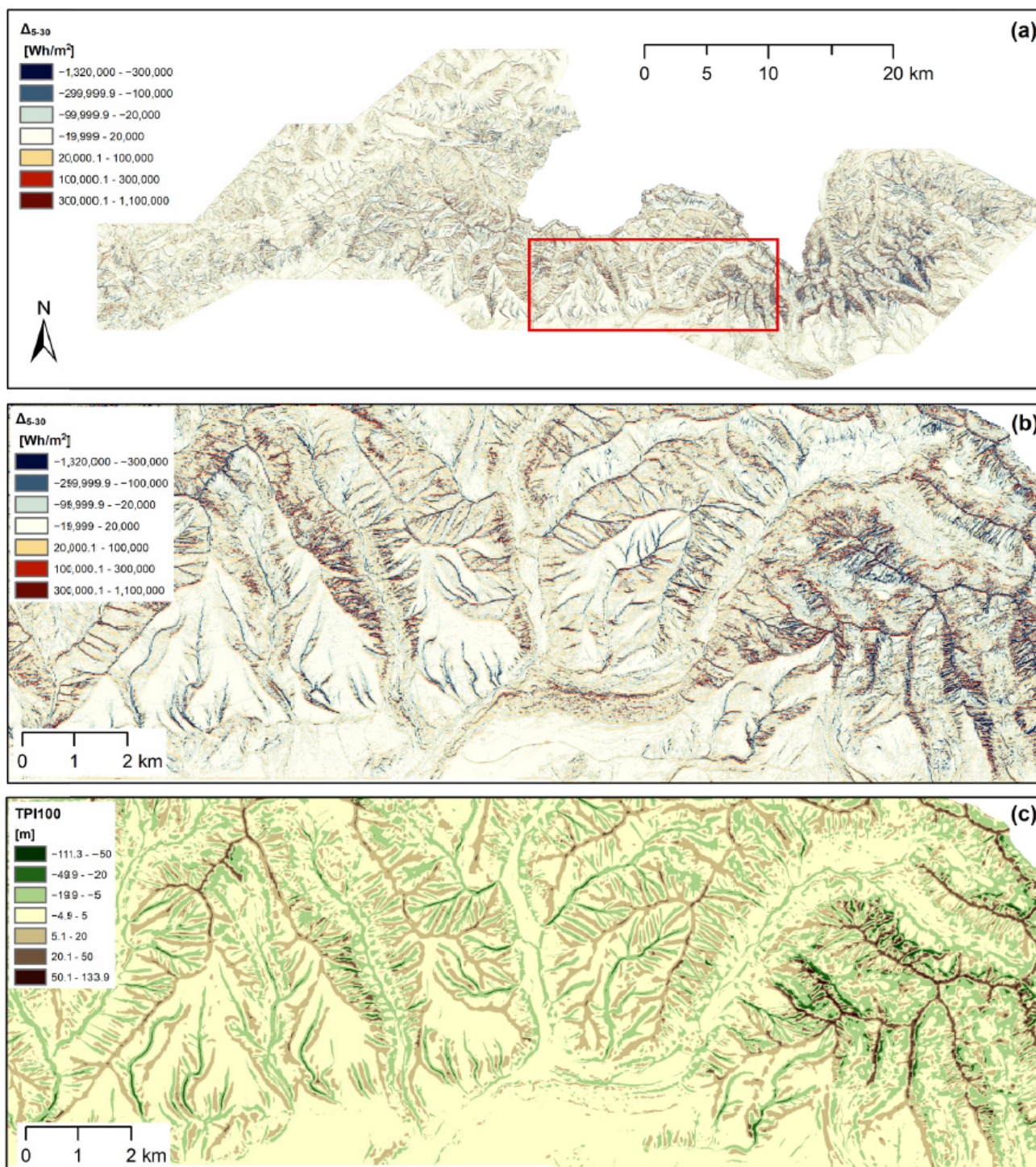


**Figure 4.** Differences between the potential solar radiation calculated at a resolution of 5 m and 30 m (a,b); TPI calculated with an input circular neighbourhood of 100 m (c). Data source: ÚGKK SR [45].

### 3.2. Correlations between Absolute Values of Potential Solar Radiation Differences and the Terrain Parameters

Potential solar radiation, slope, aspect, and TPI100, all calculated at a resolution of 5 m, are shown in Figure 5. Other TPI values are shown as their absolute values to better demonstrate their relationship with differences in potential solar radiation calculated at different resolutions (Figure 6).

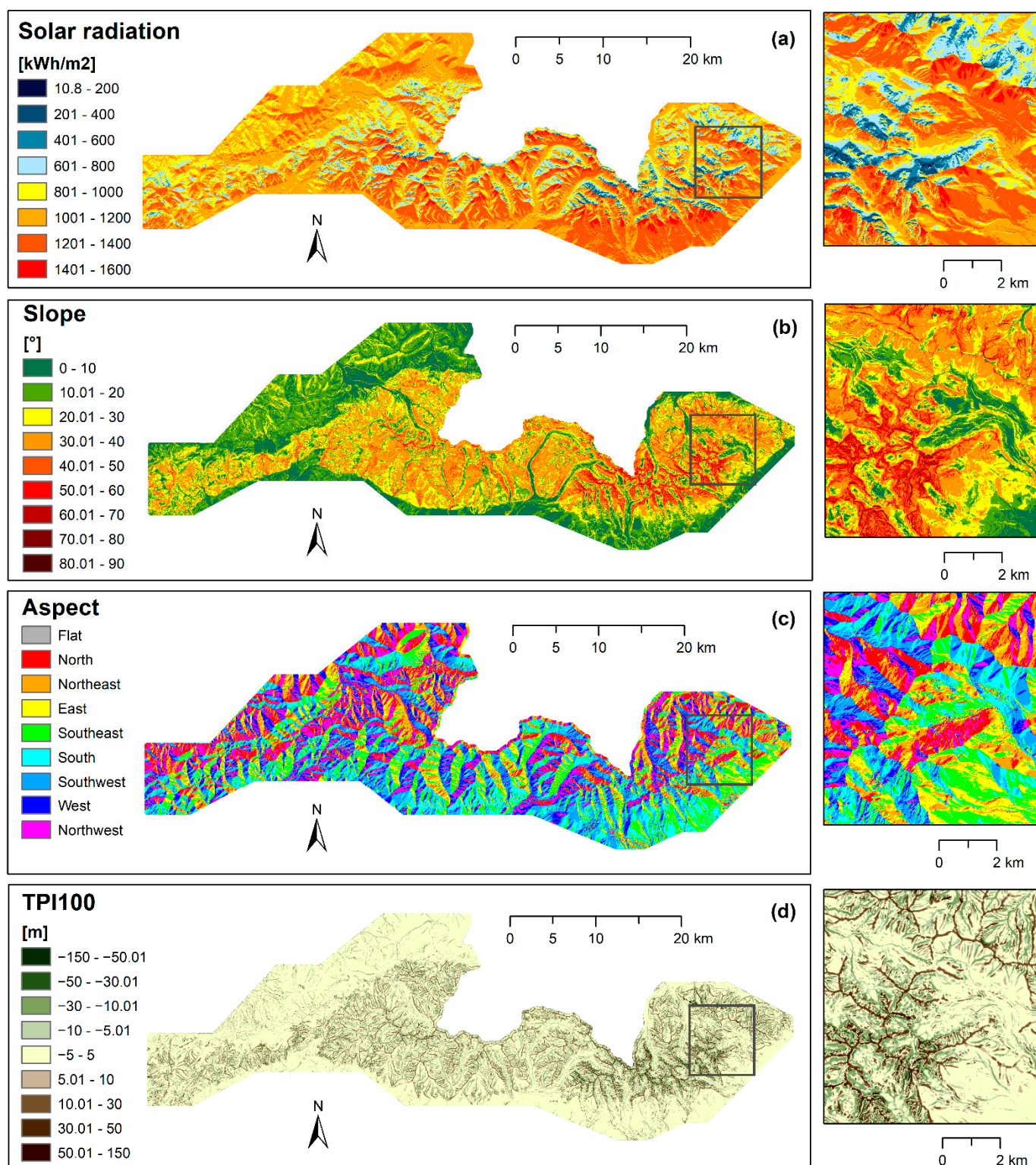


**Figure 5.** Potential solar radiation (a) and the basic terrain parameters in the Tatra Mountains: slope (b), aspect (c), and TPI100 (d) (calculated based on DTM 5.0 at a spatial resolution of 5 m). Data source: ÚGKK SR [45].

Table 4 shows the mutual correlations between absolute values of differences in the calculation of potential solar radiation at different resolutions of DEM (or errors caused by lower resolution of the DEM) and the terrain parameters, including absolute values of TPI calculated with different circular neighbourhoods (10 m–1000 m).

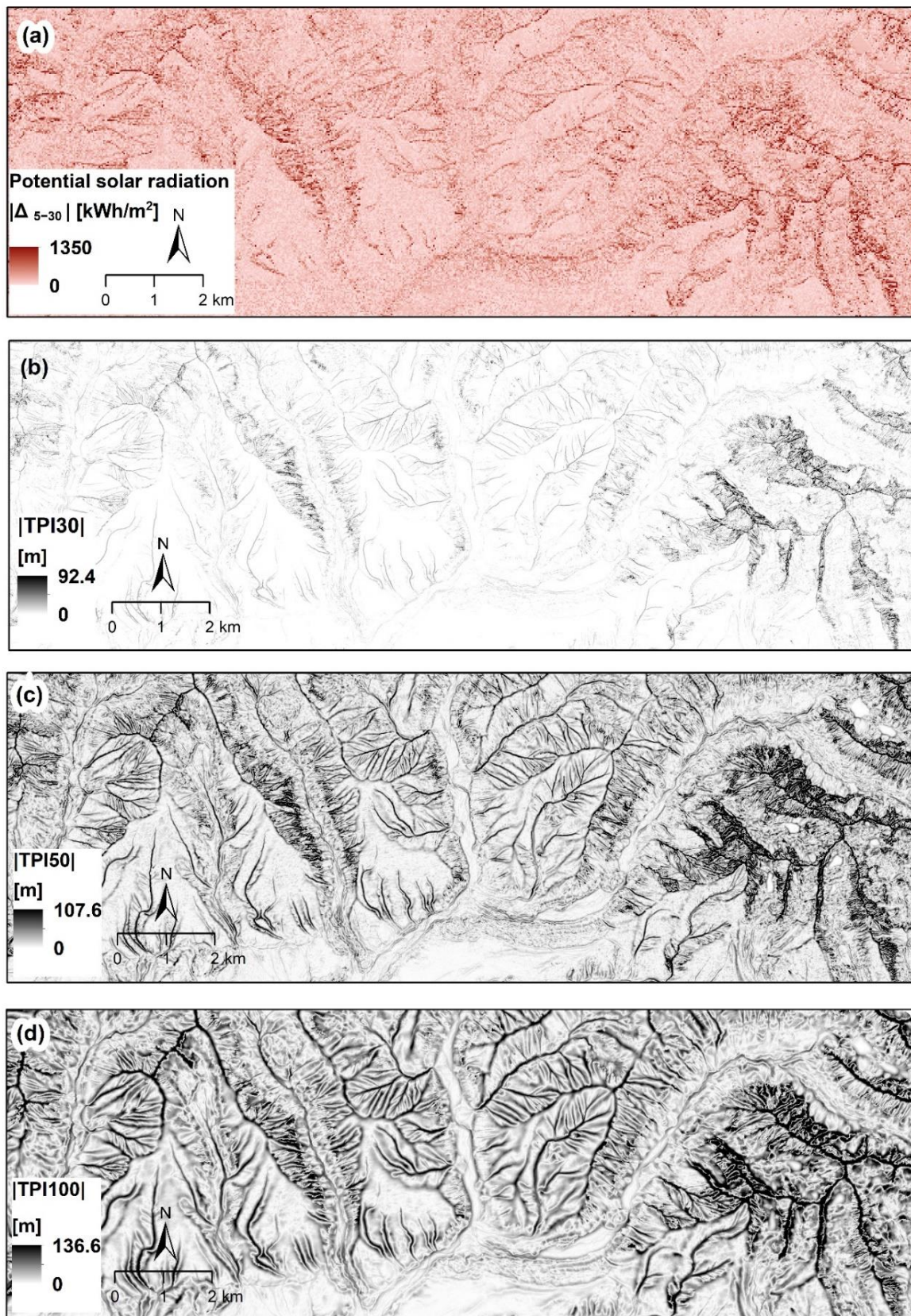


**Figure 6.** Absolute values of the differences between potential solar radiation calculated at a resolution of 5 m and 30 m (a); the absolute values of TPI calculated with a circular neighbourhood of 30 m (b), 50 m (c), and 100 m (d) based on DTM 5.0 at a spatial resolution of 5 m. Data source: ÚGKK SR [45].

**Table 4.** Mutual correlations of solar radiation differences calculated based on DEM at different resolutions (5 m vs. 10 m, 30 m, and 90 m) and the terrain parameters (elevation, |TPI1000|, |TPI500|, |TPI100|, |TPI50|, |TPI30|, |TPI10|, northness, eastness, and slope).

Terrain Parameter	$ \Delta_{5-10} ^1$ [Wh/m <sup>2</sup> ]	$ \Delta_{5-30} ^1$ [Wh/m <sup>2</sup> ]	$ \Delta_{5-90} ^1$ [Wh/m <sup>2</sup> ]
Elevation [m]	0.22	0.24	0.26
TPI1000  [m]	0.10	0.10	0.11
TPI500  [m]	0.19	0.20	0.21
TPI100  [m]	0.25	0.29	<b>0.33</b>
TPI50  [m]	<b>0.32</b>	<b>0.36</b>	<b>0.38</b>
TPI30  [m]	<b>0.39</b>	<b>0.41</b>	<b>0.40</b>
TPI10  [m]	<b>0.46</b>	<b>0.45</b>	<b>0.35</b>
Northness	0.17	0.17	0.18
Eastness	−0.01	0.00	0.01
Slope [°]	<b>0.31</b>	<b>0.35</b>	<b>0.38</b>

<sup>1</sup>  $|\Delta_{5-10}|$ ,  $|\Delta_{5-30}|$ , and  $|\Delta_{5-90}|$  indicate the absolute value of the difference in potential solar radiation calculated at a resolution of 5 m compared to the potential solar radiation calculated at a resolution of 10 m, 30 m, and 90 m, respectively. Bold indicates a moderate correlation (the highest values of correlations in our analysis).

The results indicate independence of the potential solar radiation differences on eastness; very low dependence on |TPI1000|, |TPI500|, and northness; and low dependence on elevation. Of particular interest is the low dependence on aspect (northness and eastness), on which the potential solar radiation directly depends. Conversely, the dependence on absolute values of TPI with input neighbourhoods of 10 m to 100 m is relatively high (Table 4). The correlation coefficient of these parameters reaches values of 0.33–0.46, suggesting a moderate correlation, although still sufficiently indicating the influence of TPI on errors in the calculation of potential solar radiation. The inaccuracy of its calculation on ridges and valleys also affects their surroundings, which may not be characterized by significant TPI values. Moderate correlations were also shown for slope (0.31–0.38) (Table 4).

Table 5 shows the intervals of absolute values of TPI50 and the associated RMSE of the potential solar radiation models calculated at a resolution lower than 5 m. On mountain ridges and valleys, RMSE reaches up to 326 321 Wh/m<sup>2</sup> (at resolutions of 5 m and 90 m). The most significant differences in the calculation of potential solar radiation resulting from different raster resolutions are in areas with high absolute values of TPI (for resolutions of 10 m, 30 m, or 90 m, values greater than 10 m lead to 4.7–6.2 times greater errors compared to errors in the flat area ( $|TPI10| < 5$  m)) (Table 5). A graphical representation of absolute values of TPI, together with differences in potential solar radiation (5 m vs. 30 m), is shown in Figure 6. This figure also confirms that the most considerable differences in potential solar radiation values are at and around peaks, ridges, and valleys.

**Table 5.** Root mean square error (RMSE) of the potential solar radiation models calculated at a resolution lower than 5 m in relation to absolute values of TPI50 (TPI calculated with a circular neighbourhood of 50 m).

TPI50  [m]	Number of Pixels	RMSE <sub>5-10</sub> [Wh/m <sup>2</sup> ]	RMSE <sub>5-30</sub> [Wh/m <sup>2</sup> ]	RMSE <sub>5-90</sub> [Wh/m <sup>2</sup> ]
[0, 2)	10,289,928	22,887.4	44,530.2	69,682.7
[2, 5)	9,392,989	27,501.8	53,915.5	87,586.7
[5, 10)	8,253,632	34,031.6	67,147.9	108,648.2
[10, 20)	6,059,706	45,339.0	89,942.6	141,941.4
[20, 50)	2,104,282	75,107.3	147,435.6	219,140.0
[50, 140)	131,778	142,263.2	247,364.5	326,320.5

### 3.3. Comparison of Calculated and Aggregated Models of Potential Annual Solar Radiation

The next result obtained in this study is a comparison of potential solar radiation calculated based on DEM at a resolution of 10 m, 30 m, and 90 m and values aggregated from a solar radiation model with a resolution of 5 m to a resolution of 10 m, 30 m, and 90 m, respectively. The statistical characteristics (RMSE) of the differences are shown in Table 6. Based on the results, we can confirm that it is more appropriate to aggregate solar radiation from a higher-resolution model.

**Table 6.** Comparison of the differences in potential solar radiation calculated and aggregated at a spatial resolution of 10 m, 30 m, and 90 m. The model with which these models are compared is calculated with a resolution of 5 m.

Processing Type	RMSE <sub>5-10</sub> [Wh/m <sup>2</sup> ]	RMSE <sub>5-30</sub> [Wh/m <sup>2</sup> ]	RMSE <sub>5-90</sub> [Wh/m <sup>2</sup> ]
Calculation	43,064.0	75,813.2	117,945.2
Aggregation	27,775.4	59,499.5	92,648.8

### 3.4. Model of Annual Potential Solar Radiation in the Tatra Mountains with a Cell Size of 5 m

The last result obtained in our study is the model of annual potential global solar radiation in the Tatra Mountains with a spatial resolution of 5 m (Figure 5b) or 2 m. The reference coordinate system used is S-JTSK (EPSG: 5514) with a file size of 464 MB (or 2.9 GB for a spatial resolution of 2 m). The above results (Section 3.3) indicate the suitability of this model for analyses where lower spatial resolution is sufficient.

## 4. Discussion

Based on the obtained results, we can state that the resolution of input data in the calculation of potential solar radiation in the GIS environment has a significant impact on the results, especially in areas with high absolute values of TPI calculated with small neighbourhoods (10 m–100 m). This is especially evident in high mountain areas, which contain rugged terrain. Consequently, in areas with a  $|TPI_{50}|$  or  $|TPI_{100}|$  greater than 10 m, we recommend applying a high-resolution DEM to calculate potential solar radiation. In this study, we used a model of potential annual solar radiation with a spatial resolution of 5 m. In addition, we calculated a model at a resolution of 2 m, which we did not include in the analyses in this study due to computational complexity and time-consuming calculations. However, it can be used for other follow-up analyses, especially in rugged terrain. The second reason is the fact that four different resolutions are sufficient to show the effect of resolution on the result. The authors of [13] also stated that calculating insolation can be very time-consuming. Calculations for a large DEM can take several hours, and for a very large DEM, even days [13]. Similarly, the authors of [8] points to the high computational complexity of the calculation of potential solar radiation at a high raster resolution. In comparison, for a study area of about 1 km<sup>2</sup>, the processing time was recorded with a standard model run of 01 m: 12 s, 06 m: 22 s, and 10 m: 7 s for 30 m, 5 m, and 0.50 m, respectively [8]. The calculations were performed on a Windows computer with an Intel i5 processor with four cores and eight GB of RAM. It should also be emphasized that processing time increases when using shorter time intervals.

However, it should be noted that even a file size of more than 2 GB, in this case, is a significant limit. In this context, it is also important to note that the Area Solar Radiation tool is designed only for local landscape scales, where it is generally acceptable to use one latitude value for the whole area [13]. With larger datasets, such as for states, countries, or continents, the results will differ significantly at different latitudes (greater than one degree). For this reason, it is not sufficient to use only a higher raster resolution for a calculation of a larger area. It is also necessary to divide broader geographical regions into smaller zones with different latitudes [13]. Our analysis in the Tatra Mountains was related to the elongated shape of the area with a difference in latitude of 0.22 degrees, although

with a range of longitude greater than 1 degree [51]. In this case, the error caused by the latitude setting leads to a potential solar radiation error of as much as 4000 Wh/m<sup>2</sup>.

The authors of [8] argue that the default model values of diffusivity and transmissivity lead to a substantial underestimation or overestimation of solar radiation. The authors further claim that model validation is necessary because actual values cannot be defined from atmospheric data prior to model implementation [8,57]. The values of solar radiation from meteorological stations are certainly useful for a comparison of the values of the calculated potential solar radiation. However, even the values of the modelled potential solar radiation are sufficient to perform many spatial analyses, especially if it is not necessary to know the exact values of solar radiation but rather their local changes in the area. The values calculated based on the DEM in our study are suitable for this purpose.

Therefore, we recommend using the potential annual solar radiation model calculated in this study with a resolution of 5 m (Figure 5a, Supplementary Material File S1) or higher for analysis in the Tatra Mountains (see Data Availability Statement). In the case of analyses in which a lower resolution is sufficient, the values of the calculated model can be aggregated to the required lower resolution (rather than calculating potential solar radiation with a lower resolution). We would like to add that model values need to be aggregated through the average function, not resampled, as resampling leads to less reliable values.

## 5. Conclusions

We found and confirmed that the most significant differences in the calculation of potential solar radiation resulting from different raster resolutions are in areas with high absolute values of TPI, i.e., mountainous areas (for resolutions of 10 m, 30 m, or 90 m, values greater than 10 m lead to 4–6 times greater errors compared to errors in a flat area).

According to our analysis, more accurate values of potential solar radiation at the required resolution (e.g., 30 m) are obtained by calculation at higher resolution (e.g., 5 m) and subsequent aggregation of values by the average function.

Based on the results, we recommend:

- In mountainous areas, calculate potential solar radiation at as high a resolution as possible (in a flat area, this is not necessary);
- For spatial analysis in the Tatra Mountains, we recommend using the solar radiation model proposed in this study (Figure 5a, Supplementary Materials File S1) or its aggregation at a lower resolution.

In future research, it could be useful to compare our results with the potential solar radiation calculated on the basis of SRTM at a resolution of 30 m or other DEMs used in spatial analyses in the Tatra Mountains. Another open issue is the calculation of potential solar radiation with even higher resolution, mainly due to analyses in smaller localities requiring more detailed knowledge of solar radiation.

Although our analysis was performed in a specific area, the results may be applicable to other areas. A high-spatial-resolution model of potential solar radiation can help improve the accuracy of various geological and ecological spatial analyses.

**Supplementary Materials:** The following data can be downloaded at <https://www.mdpi.com/article/10.3390/ijgi11070389/s1>, File S1: Solar\_radiation\_Tatra\_5m.zip.

**Author Contributions:** Conceptualization, Renata Ďuračiová; formal analysis, Renata Ďuračiová and Filip Pružinec; methodology, Renata Ďuračiová; project administration, Renata Ďuračiová; resources, Renata Ďuračiová; validation, Filip Pružinec; visualization, Renata Ďuračiová; writing—original draft, Renata Ďuračiová; writing—review and editing, Filip Pružinec. All authors have read and agreed to the published version of the manuscript.

**Funding:** This research was funded by grant VEGA 1/0468/20 of the Scientific Grant Agency of the Ministry of Education, Science, Research, and Sport of the Slovak Republic and the Slovak Academy of Sciences and the grant “Geoinformation analytical IoT platform for decision support”—GIANT-313022U785 under the call OPVaI-MH/DP/2018/2.2.2-20 with the support of the Ministry of Economy of the Slovak Republic, co-funded by the European Regional Development Fund.

**Institutional Review Board Statement:** Not applicable.

**Informed Consent Statement:** Not applicable.

**Data Availability Statement:** The data presented in this study are available from the corresponding author upon request, including the potential annual global solar radiation model calculated at a resolution of 2 m (2.9 GB). The potential annual global solar radiation model calculated at a resolution of 5 m is available in Supplementary Materials (131 MB). The input data are available at: [https://www.geoportal.sk/en/zbgis/als\\_dmr/](https://www.geoportal.sk/en/zbgis/als_dmr/) (accessed on 21 February 2022). The data are freely available, but the user is obliged to state the source of aerial laser scanning products when creating his own work and publishing it as follows: “ÚGKK SR”.

**Acknowledgments:** We would like to thank the Office of Geodesy, Cartography and Cadastre Authority of the Slovak Republic for the provided data.

**Conflicts of Interest:** The authors declare no conflict of interest.

## References

1. Solar Energy Technologies Office. Solar Radiation Basics. Available online: <https://www.energy.gov/eere/solar/solar-radiation-basics> (accessed on 16 December 2021).
2. Fu, Q. Solar radiation. In *Encyclopedia of Atmospheric Sciences*; Holton, J., Pyle, J., Curry, J., Eds.; Academic Press: Amsterdam, The Netherlands, 2003; pp. 1859–1863.
3. Monteith, J.L. Solar Radiation and Productivity in Tropical Ecosystems. *J. Appl. Ecol.* **1972**, *9*, 747–766. [CrossRef]
4. Leuchner, M.; Hertel, C.; Rötzer, T.; Seifert, T.; Weigt, R.; Werner, H.; Menzel, A. Solar Radiation as a Driver for Growth and Competition in Forest Stands. In *Growth and Defence in Plants. Ecological Studies (Analysis and Synthesis)*; Matyssek, R., Schnyder, H., Oßwald, W., Ernst, D., Munch, J., Pretzsch, H., Eds.; Springer: Berlin/Heidelberg, Germany, 2012; pp. 175–191. [CrossRef]
5. Olpenda, A.S.; Stereńczak, K.; Będkowski, K. Modeling Solar Radiation in the Forest Using Remote Sensing Data: A Review of Approaches and Opportunities. *Remote Sens.* **2018**, *10*, 694. [CrossRef]
6. IARC Working Group on the Evaluation of Carcinogenic Risks to Humans. *Radiation (IARC Monographs on the Evaluation of Carcinogenic Risks to Humans, No. 100D)*; International Agency for Research on Cancer: Lyon, France, 2012. Available online: <https://www.ncbi.nlm.nih.gov/books/NBK304362/> (accessed on 16 December 2021).
7. Hofierka, J.; Cebecauer, T. Spatial interpolation of elevation data with variable density: A new methodology to derive quality DEMs. *IEEE Geosci. Remote Sens. Lett.* **2007**, *4*, 117–121. [CrossRef]
8. Kausika, B.B.; van Sark, W.G.J.H.M. Calibration and validation of ArcGIS solar radiation tool for photovoltaic potential determination in the Netherlands. *Energies* **2021**, *14*, 1865. [CrossRef]
9. Fuentes, J.E.; Moya, F.D.; Montoya, O.D. Method for Estimating Solar Energy Potential Based on Photogrammetry from Unmanned Aerial Vehicles. *Electronics* **2020**, *9*, 2144. [CrossRef]
10. Tovar-Pescador, J.; Pozo-Vazquez, D.; Ruiz-Arias, J.A.; Batlles, J.; Lopez, G.; Bosch, J.L. On the use of the digital elevation model to estimate the solar radiation in areas of complex topography. *Meteorol. Appl.* **2006**, *13*, 279–287. [CrossRef]
11. Arnold, N.; Rees, G. Effects of digital elevation model spatial resolution on distributed calculations of solar radiation loading on a High Arctic glacier. *J. Glaciol.* **2009**, *55*, 973–984. [CrossRef]
12. ESRI. ArcGIS Desktop. An Overview of the Solar Radiation Toolset. Available online: <https://desktop.arcgis.com/en/arcmap/latest/tools/spatial-analyst-toolbox/an-overview-of-the-solar-radiation-tools.htm> (accessed on 16 December 2021).
13. ESRI. ArcGIS Desktop. Area Solar Radiation. Available online: <https://desktop.arcgis.com/en/arcmap/latest/tools/spatial-analyst-toolbox/area-solar-radiation.htm> (accessed on 16 December 2021).
14. GRASS GIS 8.0.1dev Reference Manual r.sun—Solar Irradiance and Irradiation Model. Available online: <https://grass.osgeo.org/grass80/manuals/r.sun.html> (accessed on 16 December 2021).
15. Hofierka, J.; Šúri, M. The solar radiation model for Open source GIS: Implementation and applications. In Proceedings of the Open Source GIS-GRASS Users Conference, Trento, Italy, 11–13 September 2002; p. 19.
16. Fu, P.A. *Geometric Solar Radiation Model with Applications in Landscape Ecology*; University of Kansas: Lawrence, KS, USA, 2000.
17. Fu, P.; Rich, P.M. A geometric solar radiation model with applications in agriculture and forestry. *Comput. Electron. Agric.* **2002**, *37*, 25–35. [CrossRef]
18. Fu, P.; Rich, P.M. *The Solar Analyst 1.0 Manual; Helios Environmental Modeling Institute (HEMI)*; University of Kansas: Lawrence, KS, USA, 2000; p. 49. Available online: [http://professorpaul.com/publications/fu\\_rich\\_2000\\_solaranalyst.pdf](http://professorpaul.com/publications/fu_rich_2000_solaranalyst.pdf) (accessed on 14 February 2022).
19. Fu, P.; Rich, P.M. Design and implementation of the solar analyst: An ArcView extension for modeling solar radiation at landscape scales. In Proceedings of the 19th Annual ESRI User Conference, San Diego, CA, USA, 26–30 July 1999; pp. 1–33. Available online: <http://www.esri.com/library/userconf/proc99/proceed/papers/pap867/p867.htm> (accessed on 14 February 2022).
20. Hetrick, W.A.; Rich, P.M.; Barnes, F.J.; Weiss, S.B. GIS-based solar radiation flux models. In *American Society for Photogrammetry and Remote Sensing Technical Papers, Photogrammetry and Modeling*; 1993; Volume 3, pp. 132–143. Available online: [http://professorpaul.com/publications/hetrick\\_et\\_al\\_1993\\_asprs.pdf](http://professorpaul.com/publications/hetrick_et_al_1993_asprs.pdf) (accessed on 14 February 2022).

21. Choi, Y.; Suh, J.; Kim, S.M. GIS-based solar radiation mapping, site evaluation, and potential assessment: A review. *Appl. Sci.* **2019**, *9*, 1960. [CrossRef]
22. Šúri, M.; Hofierka, J. A new GIS-based solar radiation model and its application to photovoltaic assessments. *Trans. GIS* **2004**, *8*, 175–190. [CrossRef]
23. Liang, J.; Gong, J.; Xie, X.; Sun, J. Solar3D: An open-source tool for estimating solar radiation in urban environments. *ISPRS Int. J. Geo-Inf.* **2020**, *9*, 524. [CrossRef]
24. Liang, J.; Gong, J.; Zhou, J.; Ibrahim, A.N.; Li, M. An open-source 3D solar radiation model integrated with a 3D Geographic Information System. *Environ. Model. Softw.* **2015**, *64*, 94–101. [CrossRef]
25. Hofierka, J.; Zlocha, M. A New 3-D Solar Radiation Model for 3-D City Models. *Trans. GIS* **2012**, *16*, 681–690. [CrossRef]
26. Hofierka, J.; Kaňuk, J.; Gallay, M. The Spatial Distribution of Photovoltaic Power Plants in Relation to Solar Resource Potential: The Case of the Czech Republic and Slovakia. *Morav. Geogr. Rep.* **2014**, *22*, 26–33. [CrossRef]
27. Bolibok, L.; Brach, M. Application of LiDAR data for the modeling of solar radiation in forest artificial gaps—A case study. *Forests* **2020**, *11*, 821. [CrossRef]
28. Kaňuk, J.; Zubal, S.; Šupinský, J.; Šašak, J.; Bombara, M.; Sedlák, V.; Gallay, M.; Hofierka, J.; & Onáčillová, K. Testing of V3.sun module prototype for solar radiation modelling on 3D objects with complex geometric structure. *Int. Arch. Photogramm. Remote Sens. Spat. Inf. Sci.-ISPRS Arch.* **2019**, *42*, 35–40. [CrossRef]
29. Mezei, P.; Jakuš, R.; Blaženec, M.; Belánová, S.; Šmídt, J. The relationship between potential solar radiation and spruce bark beetle catches in pheromone traps. *Ann. For. Res.* **2012**, *55*, 243–252. Available online: <https://afrjournal.org/index.php/afr/article/view/64> (accessed on 14 February 2022).
30. Mezei, P.; Potterf, M.; Škvarenina, J.; Rasmussen, J.G.; Jakuš, R. Potential solar radiation as a driver for bark beetle infestation on a landscape scale. *Forests* **2019**, *10*, 604. [CrossRef]
31. Van der Zande, D.; Stuckens, J.; Verstraeten, W.W.; Mereu, S.; Muys, B.; Coppin, P. 3D modeling of light interception in heterogeneous forest canopies using ground-based LiDAR data. *Int. J. Appl. Earth Obs. Geoinf.* **2011**, *13*, 792–800. [CrossRef]
32. Redweik, P.M.; Catita, C.; Brito, M.C. 3D local scale solar radiation model based on urban LiDAR data. *Int. Arch. Photogramm. Remote Sens. Spat. Inf. Sci.* **2012**, XXXVIII-4/W19, 265–269. [CrossRef]
33. Bode, C.A.; Limm, M.P.; Power, M.E.; Finlay, J.C. Subcanopy Solar Radiation model: Predicting solar radiation across a heavily vegetated landscape using LiDAR and GIS solar radiation models. *Remote Sens. Environ.* **2014**, *154*, 387–397. [CrossRef]
34. Öhrn, P. *The Spruce Bark Beetle Ips Typographus in a Changing Climate—Effects of Weather Conditions on the Biology of Ips Typographus. Introductory Research Essay No 18*; Swedish University of Agricultural Sciences: Uppsala, Sweden, 2012; p. 27. Available online: [https://pub.epsilon.slu.se/8619/1/ohrn\\_p\\_120320.pdf](https://pub.epsilon.slu.se/8619/1/ohrn_p_120320.pdf) (accessed on 14 February 2022).
35. Mezei, P.; Grodzki, W.; Blaženec, M.; Jakuš, R. Factors influencing the wind-bark beetles' disturbance system in the course of an Ips typographus outbreak in the Tatra Mountains. *For. Ecol. Manag.* **2014**, *312*, 67–77. [CrossRef]
36. Chen, H.; Jackson, P.L. Spatiotemporal mapping of potential mountain pine beetle emergence—Is a heating cycle a valid surrogate for potential beetle emergence? *Agric. For. Meteorol.* **2015**, *206*, 124–136. [CrossRef]
37. Jeniček, M.; Pevná, H.; Ondrejka, M. Canopy structure and topography effects on snow distribution at a catchment scale: Application of multivariate approaches. *J. Hydrol. Hydromech.* **2018**, *66*, 43–54. [CrossRef]
38. Sproull, G.J.; Adams, M.; Bukowski, M.; Krzyzanowski, T.; Szewczyk, J.; Statwick, J.; Szwagrzyk, J. Tree and stand-level patterns and predictors of Norway spruce mortality caused by bark beetle infestation in the Tatra Mountains. *For. Ecol. Manag.* **2015**, *354*, 261–271. [CrossRef]
39. Kissiyar, O.; Blaženec, M.; Jakuš, R.; Willekens, A.; Ježík, M.; Baláž, P.; Valckenborg, J.V.; Celer, S.; Fleischer, P. TANABBO model—A remote sensing based early warning system for forest decline and bark beetle outbreaks in Tatra Mts.—Overview. In *GIS and Databases in the Forest Protection in Central Europe*; Grodzki, W., Ed.; Centre of Excellence PROFEST at the Forest Research Institute: Warsaw, Poland, 2005; pp. 15–34.
40. Jakuš, R.; Ježík, M.; Kissiyar, O.; Blaženec, M. Prognosis of bark beetle attack in TANABBO model. In *GIS and Databases in the Forest Protection in Central Europe*; Grodzki, W., Ed.; Centre of Excellence PROFEST at the Forest Research Institute: Warsaw, Poland, 2005; pp. 35–44.
41. Rodriguez, E.; Morris, C.S.; Belz, J.E.; Chapin, E.C.; Martin, J.M.; Daffer, W.; Hensley, S. *An Assessment of the SRTM Topographic Products*; Technical Report JPL D-31639; Jet Propulsion Laboratory: Pasadena, CA, USA, 2005; p. 143.
42. Farr, T.G.; Rosen, P.A.; Caro, E.; Crippen, R.; Duren, R.; Hensley, S.; Kobrick, M.; Paller, M.; Rodriguez, E.; Roth, L.; et al. The Shuttle Radar Topography Mission. *Rev. Geophys.* **2007**, *45*, RG2004. [CrossRef]
43. Shuttle Radar Topography Mission (SRTM). Available online: <https://www2.jpl.nasa.gov/srtm/> (accessed on 18 February 2022).
44. UNESCO. Tatra Transboundary Biosphere Reserve, Poland/Slovakia. Available online: <https://en.unesco.org/biosphere/eu-na/tatra> (accessed on 21 February 2022).
45. Geoportál. Airborne Laser Scanning and DTM 5.0. Available online: [https://www.geoportal.sk/en/zbgis/als\\_dmr/](https://www.geoportal.sk/en/zbgis/als_dmr/) (accessed on 21 February 2022).
46. OSM-Boundaries. Available online: <https://osm-boundaries.com/> (accessed on 6 July 2022).
47. OpenStreetMap. Copyright and Licence. Available online: <https://www.openstreetmap.org/copyright/en> (accessed on 6 July 2022).
48. Slovak Hydrometeorological Institute. Available online: <https://www.shmu.sk/en/> (accessed on 21 February 2022).

49. Global Solar Atlas. Available online: <https://globalsolaratlas.info> (accessed on 21 February 2022).
50. ZB GIS Map Client. Terrain. Available online: <https://zbgis.skgeodesy.sk/mkzbgis/en/teren> (accessed on 21 February 2022).
51. Parameters for ALS Data Collection Lots. Available online: <https://www.geoportal.sk/files/zbgis/lls/parameters-als-data-collection-lots.pdf> (accessed on 21 February 2022).
52. ESRI. ArcGIS Desktop. Resample. Available online: <https://desktop.arcgis.com/en/arcmap/latest/tools/data-management-toolbox/resample.htm> (accessed on 17 May 2022).
53. Roberts, D.W. Ordination on the basis of fuzzy set theory. *Vegetatio* **1986**, *66*, 123–131. [CrossRef]
54. Weiss, A.D. Topographic Position and Landforms Analysis. Available online: [http://www.jennessent.com/downloads/tpi-poster-tnc\\_18x22.pdf](http://www.jennessent.com/downloads/tpi-poster-tnc_18x22.pdf) (accessed on 21 February 2022).
55. Jenness, J. Topographic Position Index (TPI) v. 1.2. (tpi\_jen.avx). Available online: [http://www.jennessent.com/downloads/tpi\\_documentation\\_online.pdf](http://www.jennessent.com/downloads/tpi_documentation_online.pdf) (accessed on 21 February 2022).
56. ESRI. ArcGIS Desktop. Available online: <https://www.esri.com/en-us/arcgis/products/arcgis-desktop/overview> (accessed on 21 February 2022).
57. Gueymard, C.A. Clear-sky irradiance predictions for solar resource mapping and large-scale applications: Improved validation methodology and detailed performance analysis of 18 broadband radiative models. *Sol. Energy* **2012**, *86*, 2145–2169. [CrossRef]